Study of Mechanical Properties of Carbon Steel Plate SA-516 Gr. 70 Welded by SAW Using V-Shape Joint Design

Samir A. Amin [a]*, **Mohannad Y. Hanna** [b], **Abdulaziz S. Khider** [c]*

[a] Mechanical Engineering Department, University of Technology-Iraq. alrabiee2002@yahoo.com

[b] Department of Mechanical Engineering, University of Technology-Iraq. 20095@uotechnology.edu.iq

[c] Mechanical Engineering Department, University of Technology-Iraq. abdulaziz.saud87@gmail.com

*Corresponding author.

A B S T R A C T

Submerged arc welding (SAW) is a fusion type welding and it is considered one of the most important welding types due to its inherent capabilities of high welding speed, high deposition rate, welding large thickness plates owing to its deep penetration characteristic and many other advantages. In this study, the goal was to investigate the effect of welding parameters, namely (welding current and welding speed) as well as the joint design on the mechanical properties (yield stress, bending force on the face of the weldment and hardness of the weld metal. Experiments were conducted employing Design of Expert (DOE) software and Response Surface Methodology (RSM) technique. The experiments were conducted by welding ASME SA-516 Gr. 70 steel plate with dimension (300 mm × 150 mm × 10 mm) depending upon the design matrix developed via the DOE. Results manifested that the optimum process parameters for maximum yield stress, maximum bending force and minimum hardness were at (425 amps) welding current and (35 cm/min) welding speed, where the arc voltage was held constant at (37 volts). The optimum values for the yield stress, bending force and hardness were (474.447 MPa, 36.997 kN and 150 HV), respectively. Finally, it was found that the predicted and experimental results of yield stress, bending force and hardness agree very well according to the ultimate error (1.05%, 1.92%, and 4.25 %), respectively.

1. Introduction

A large number of works has been done by many researchers in the field of submerged arc welding. This paper briefly covers the previously published works carried out by researchers in the various fields concerning with the experimental investigation, modeling and optimization of SAW process

parameters that have effect on the mechanical properties. The tensile strength properties and hardness of the welded joints increase with the increase in number of passes. In the contrary, the ductility and toughness decreases gradually. These changes in mechanical behavior can be related to the observed microstructural properties, particularly the amount of morphology and the ferrite delta distribution [1]. The deposition rate increases greatly with the increase in welding speed at all values of heat inputs investigated, without affecting the weldment soundness. Hardness values decrease with an increase in welding speed and heat input [2]. With the formation of acicular ferrite, the ultimate tensile strength and yield strength of weld metal increases for fluxes containing TiO_2, the inclusion percentage of welds reduces the area of reduction and elongation percentages [3]. It was deduced that the weld metal grain structure and heat affected zone are affected by the heat input. Both the ultimate tensile strength and yield strength decreased with the increase in heat input, while the percentage elongation has increased [4]. The testing results showed the significance of cladding methods and estimated heat treatment influences on stated mechanical properties. The microhardness increased with the decrease in heat input, also it was found that the percentage of graphite and slow cooling rate) which result in better mechanical properties [5]. It was found that the high cooling rate and low heat input caused the higher hardness [6]. The results depicted that the current had a significant effect on the hardness, where with the increase of welding current from 300 A to 330 A, the hardness decreased [7]. The speed of welding and the arc voltage possess an important influence upon the residual stress. The speed of welding mostly raised the residual stresses over the entire chosen levels of input [8]. The results revealed that the microhardness decrease significantly with the increase in welding current [9].

From the previous works they can be concluded that a lot of works were done for the optimization of mechanical properties, where they have taken the effect of number of passes of welding, type/amount of inclusions and the evolution of weld microstructure, influence of flux chemical composition, addition of alloying element powder (nickel and molybdenum), TiO_2 addition to the flux composition and many other effects. Nevertheless, a little work considered the modeling and optimization the effect of welding parameters in SAW pressure vessel materials on their mechanical properties, experimentally and theoretically. Accordingly, the objective of the present paper is first to study the effect of using the submerged arc welding parameters, including current, welding speed with the use of V-shape joint design on the mechanical properties of low carbon steel plate SA-516 Gr. 70 that is usually utilized for manufacturing pressure vessels. Design of Experiment (DOE) is used to model and optimize the input welding parameters together with the outputs including yield stress, maximum bending force and hardness of the SAW specimens for comparing the predicted results with the experimental ones.

2. Experimental Work

I. Material

The base material used in the welding process was low carbon steel plate (ASME SA-516 Gr. 70) with a thickness of 10 mm; it is usually employed for producing tanks in the petroleum industry, boilers, and pressure vessels. All plates were submerged welded utilizing ASME SFA-5.17M EM12K wire (3.25 mm diameter) and ASME SFA-5.17M F48A2 flux having 0.8 basicity index [10]. Table 1 lists the chemical analyses of the used and nominal ASME SA-516 Gr. 70 for a plate thickness of less than (12.5 mm), and Table 2 depicts their mechanical properties for the purposes of comparison and conformity. In addition, the chemical composition of the used and nominal of ASME SFA-5.17M EM12K is given in Table 3.

Table 1: Chemical compositions of nominal and used steel plate (ASME SA-516 Gr. 70) [11]

Material wt.%	%C Max	%Mn	%Si	%P Max	%S Max
Nominal (for, t ≤ 12.5 mm)	0.27	0.79/1.3	0.13/0.45	0.035	0.035
Used	0.22	1.31	0.3	---	---

Table 2: Mechanical properties of nominal and used steel plate (ASME SA-516 Gr. 70) [11]

	Tensile strength Mpa	Yield strength MPa	Elongation (%)	Bending Force KN	Hardness HV
Nominal	485/620	260 (min)	21 (min)	---	---
Used	520	385	35	36	160

Table 3: Chemical composition of nominal and used electrode wire

	Materials wt. %					
	%C	**%Mn**	**%Si**	**%P**	**%S**	**%Cu**
Nominal [10]	**0.05/0.15**	**0.8/1.25**	**0.1/0.35**	**0.03** (max)	**0.03** (max)	**0.35** (max)
Used [12]	**0.07**	**1.0**	**0.15**	**---**	**0.025**	**---**

II. Submerged arc welding conditions

To investigate the influence of the input factors on the mechanical properties developed via the process of SAW, two welding factors (current in ampere and travel speed in cm/min) were utilized as an individual factor with five levels as shown in the Table 4. These levels were chosen depending upon the actual practices that used in the Heavy Engineering Equipment State Company (HEESCo).

III. Welding procedure

First, the plate was cut to (26) pieces having dimensions (300×150×10 mm), and their surfaces were then cleaned for the oxides and contamination removal via the sand blasting. Milling cutter was used to make the V-groove with $60^°$ angle (included angle) of single butt weld joint and then submerged arc welded to make (13) specimens. Milling cutter was utilized to produce a groove having (V) shape with $60^°$ included angle in a single-butt weld joint that then submerged arc welded to make (13) specimens. All the experiments were achieved depending upon on the matrix of design matrix (Table 5) made via the DOE software (Version 10) with five levels of input factors for finding out their effect on the mechanical properties and hardness induced in the SAW process. Figure 1 shows a simple schematic of the type of joint design used in the experiment. Figure 2 displays the used welding machine, type (EsabA2 Multitrack with the A2-A6 process controller PEK).

Table 4: Used levels of input factors

Input parameter	Levels				
	-2	**-1**	**0**	**+1**	**+2**
Welding current (Ampere)	275	325	375	425	475
Welding speed (cm/min)	20	25	30	35	40

Table 5: Experimental design matrix for both actual input factors and responses

| Std. No.	Welding Current (Ampere)	Welding Speed (cm/min)	Yield Stress (MPa)	Maximum Bending Force (kN)	Hardness (HV)
1	325	25	453.39	37.32	206.65
2	425	25	423.69	40.88	195.30
3	325	35	489.91	35.36	180.65
4	425	35	479.47	37.72	143.95
5	275	30	472.44	35.20	206.54
6	475	30	425.43	39.48	173.00
7	375	20	415.61	43.64	207.10
8	375	40	490.56	36.20	154.11
9	375	30	486.32	36.80	180.15
10	375	30	488.87	35.74	172.56
11	375	30	475.69	35.80	182.26
12	375	30	485.57	35.84	176.75
13	375	30	480.17	35.60	174.65
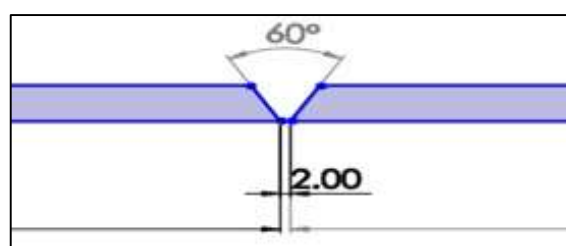
Figure 1: A simple schematic of joint design used in the experiment

Figure 2: EsabA2 Multitrack with the A2-A6 process controller PEK

IV. Measurements of yield stress, maximum bending force and hardness

All the tensile and bending tests were conducted in the Department of Production Engineering and Metallurgy at the University of Technology using WDW-200E Testing machine. The average of yield stress and max bending force was taken from two tests, as listed in Table 5. Hardness measurements were carried out at the Department of Mechanical Engineering at the University of Technology using LARYEE HBRVS testing machine on a polished surface specimen at the neutral axis of the weld metal only, taking the mean of three readings as given in Table 5.

V. Design of experiments

In the current investigation, the RSM approach was employed for developing mathematical model depending upon the experimental results. Quadratic functions of the response surface must be regarded, since the curvature may be insufficiently modeled via employing the first-order function during the ranges of the common working states. 13 experiments were conducted depending upon the experimental design matrix. The tests were carried out randomly at various coded levels from (-2) to (+2) utilized with each factor, where each used level corresponded to an actual value adapted to the coded one. Therefore, the welding input factors investigated include the current and the travel speed. The experimental design matrix employed for the input factors with the resulted output (response) values is elucidated in the Table 5. The prediction model with a 95% confidence level was established via "DESIGN EXPERT Version 10".

3. Results and Discussion

I. Modeling of yield stress

The proper model was first chosen and made via employing the approach of RSM, and then the characteristics of the response were utilized to determine the regression expressions to the model. The experimental results given in Table 5 were employed to make the regression expressions, which were drawn to explore the process factors effect on the various characteristics of response. Analysis of variance (ANOVA) for the response surface quadratic model for yield stress was achieved with backwards elimination of insignificant coefficients for analyzing statistically the results, as given in the Table 6.
The F-value of (50.40) of the model shown in the Table 6 depicts that the model is 'significant' with 95% confidence level. The "Prob> F" values less than (0.05) indicate that the terms of this model are important. In such case, the terms (A, B, A² and B²) are significant ones in such model. Thus, such model explains that the current (A) of welding, speed (B) of welding and their squared terms possess the largest impact on the yield stress. In addition, the lack of fitting refers to a good model.
The tentative quadratic predicted model established for yield stress induced in the SAW of (ASME SA-516 Gr. 70) low carbon steel is given as follows:
Yield stress = - 320.03445 + 2.38429 * Current + 22.40980 * Welding speed - 3.47719E-003 * Current^2 - 0.30622 * Welding speed^2 (1)
The model adequacy checking was performed via the analysis of residual, and the outputs are evinced in the Figures 3 and 4, respectively. The plot of normal probability is presented in Figure 3. The errors are distributes normally as appeared in such figure, where the residuals exist on a straight line. The standardized residuals relevant to the predicted results are shown in the Figure 4.

Table 6: ANOVA for response surface quadratic model for yield stress

Source	Sum of Squares	df	Mean Square	F Value	P-value Prob > F
Model	8790.42	4	2197.61	50.40	< 0.0001 significant
A-Current	466.23	1	466.23	10.69	0.0114
B-Welding speed	4888.40	1	4888.40	112.12	< 0.0001
A^2	1731.53	1	1731.53	39.71	0.0002
B^2	1342.88	1	1342.88	30.80	0.0005
Residual	348.81	8	43.60		
Lack of Fit	235.81	4	58.95	2.09	0.2469 not significant
Pure Error	113.00	4	28.25		
Cor Total	9139.23	1 2			
Std. Dev.	6.6		R-Squared		0.9618
Mean	466.7		Adj. R-Squared		0.9428
C.V. %	1.41		Pred. R-Squared		0.8591
PRESS	1287.72		Adeq. Precision		21.002
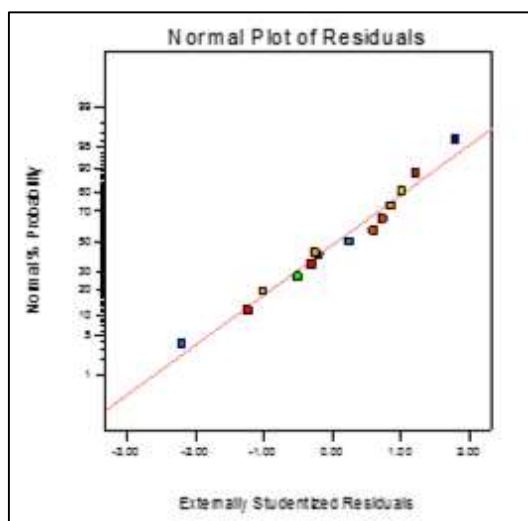
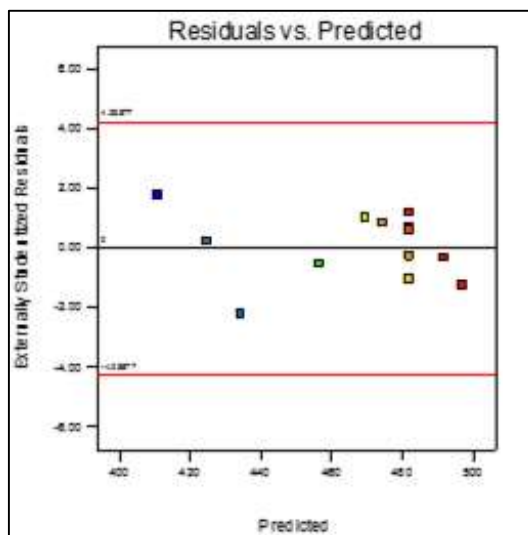**Figure 3: Normal distribution of yield stress data**

Figure 4: Residual versus predicted data

The residuals do not appear any explicit unfamiliar style and are distributed in both positive and negative direction. This demonstrates the adequacy of the model. Figure 5 illustrates that the yield stress predicted results are close to the actual ones that measured in tests, explaining that both predicted and experimental outputs possess a good agreement. This output is confirmed via the (2D)

contour graph and (3D) surface graph displayed in Figures 6 and 7, respectively in terms of current and travel speed of welding.
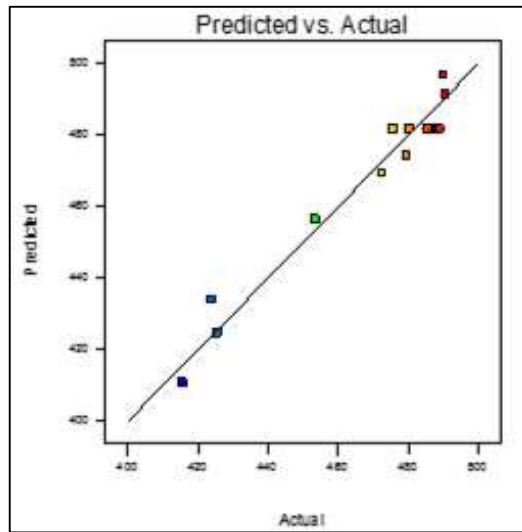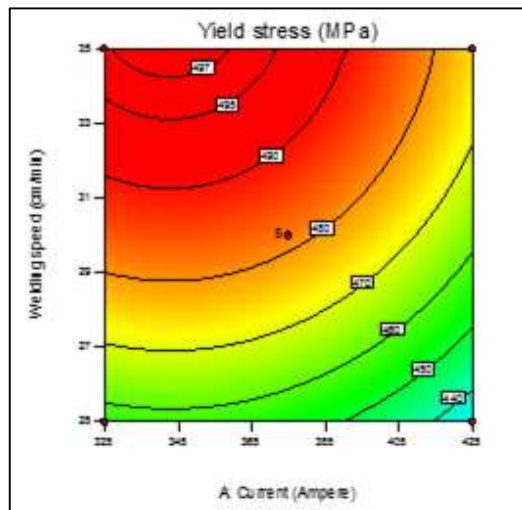

Figure 5: Predicted versus actual data

Figure 6: 2D contour graph of yield stress as a function of welding speed and welding current
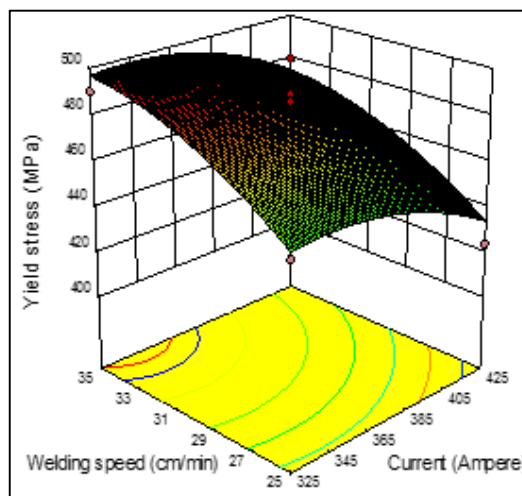

Figure 7: 3D surface plot of yield stress as a function of welding speed and welding current

It can be seen from figure 6 that increasing the welding speed caused greater influence on yield stress than the current. This is attributed to that at higher welding speed there is no more opportunity to

result more heat to soften the welded joint, therefore increasing yield stress. This is confirmed by Figure 7 showing that the maximum yield stress occurred at the highest level of welding speed (35 cm/min) and the lowest level of current (325 Ampere). This is in agreement with ref. [4]. This result is likely attributed to effect that increasing the welding speed at lower current resulted less thermal effect on the material, thus increasing the yield stress. However, the influence of current is obviously less than that for welding speed on yield stress during welding over all used levels (Figure 7).

II. Modeling of maximum bending force

In a similar way, for the maximum bending force for the face of the weld results given in table 5, a decreased quadratic model in the coded terms was analyzed using the backwards elimination of the unimportant coefficients. Table 7 reveals the statistical analysis of variance (ANOVA), and this model is significant at 95% confidence. In such model, the welding speed (B) and the squared terms (A²) and (B²) are all significant. This model explains that these three terms possess the greatest impact on the maximum bending force. In addition, there is no interaction between the current and welding speed. In addition, the lack of fitting test refers to a good model.

The final equation of maximum bending force (face) in terms of the actual factors is:

Maximum bending force $= + 93.02808 - 0.082393 * \text{Current} - 2.73354 * \text{Welding speed} + 1.42034E\text{-}004 * \text{Current}^2 + 0.040003 * \text{Welding speed}^2$ (2)

For checking statistically, the adequacy of this model, the plot of the normal probability of residuals (Figure 8) for the max bending force results showed that generally the residuals (errors) fall on a straight line and they are distributed normally. Also, there are no clear patterns or uncommon structure, implying accurate models. The standardized residuals relevant to the predicted results are shown in the Figure 9. The residuals do not appear any explicit uncommon style and are distributed in both positive and negative direction. This clarifies the adequacy of the model. Figure 10 shows the predicted versus the actual data for comparison purpose.

Referring to the Figure 11 for the (2D) contour plot, one can note that, generally, the maximum bending force has the highest value at a higher level of welding current and lower value of welding speed due to high deposition rate on the face of the weld. It can also be seen that at the higher current and higher welding speed the bending force decreases. Where, Figure 12 manifests the (3D) plot of bending force in terms of welding current and travel speed and confirms that the increment of arc current remained the maximum bending force constant at a lower level of welding speed, while the increase of welding speed decreases the maximum bending force at lower and higher level of welding current. However, the welding current is not influential during welding over the used range of its levels.

III. Modeling of hardness

The average responses obtained for hardness were utilized in the calculation of the models of response surface per response employing the method of the least squares. For the hardness prediction, a decreased quadratic model in the coded terms was analyzed via the backwards elimination of unimportant coefficients. This model reveals that the terms (A), the interaction (AB) and (A²) are significant. This means that these three terms (welding current and the interaction of both current and welding speed) have the highest impact on hardness. Table 8 manifests the statistical analysis of variance (ANOVA) produced by the software for the rest of terms. This model is significant with 95% confidence level. The lack of fitting test indicates a good model.

Table 7: ANOVA for response surface quadratic model for maximum bending force (Face)

Source	Sum of Squares	df	Mean Square	F Value	P-value Prob > F
Model	73.85	4	18.46	43.50	< 0.0001 significant
A-Current	0.042	1	0.042	0.099	0.7611
B-Welding speed	33.33	1	33.33	78.55	< 0.0001
A^2	2.89	1	2.89	6.81	0.0312
B^2	22.92	1	22.92	54.00	< 0.0001
Residual	3.40	8	0.42		
Lack of Fit	2.47	4	0.62	2.68	0.1817 not significant
Pure Error	0.92	4	0.23		

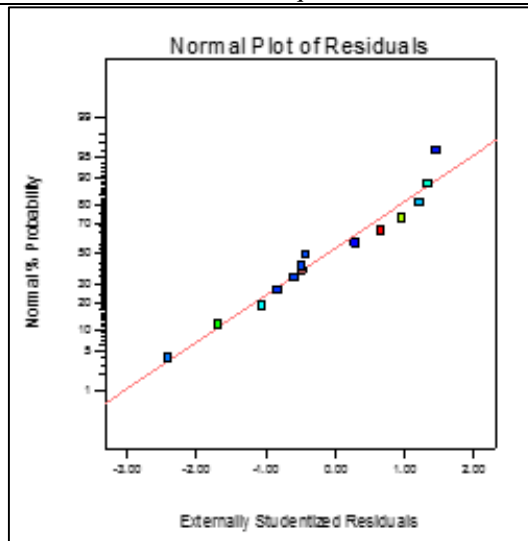| Cor Total	77.24	12		
Std. Dev.	0.65		R-Squared	0.9560
Mean	37.35		Adj. R-Squared	0.9341
C.V. %	1.74		Pred. R-Squared	0.7693
PRESS	17.82		Adeq. Precision	21.910

Figure 8: Normal distribution of maximum bending force data
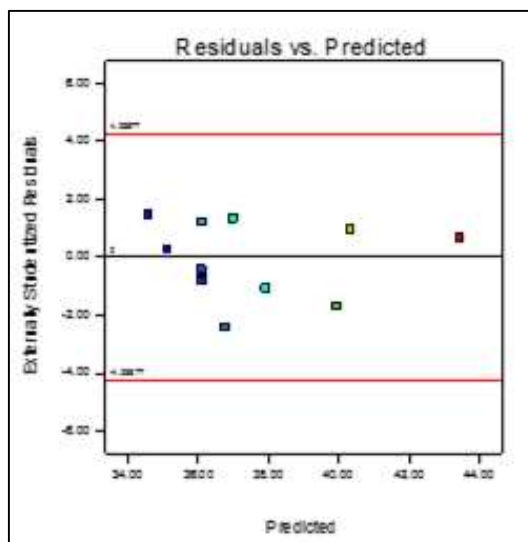
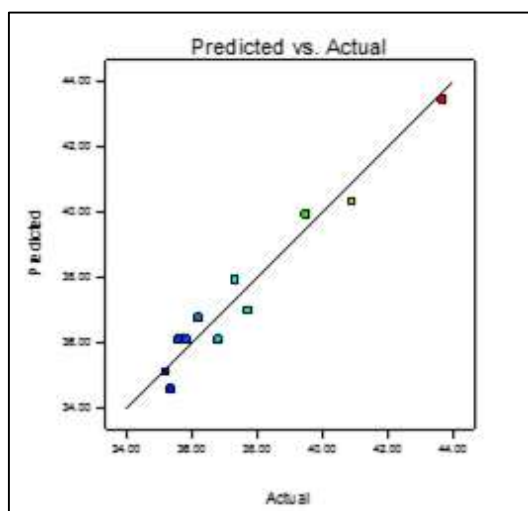**Figure 9: Residual versus predicted data**

Figure 10: Predicted vs. Actual

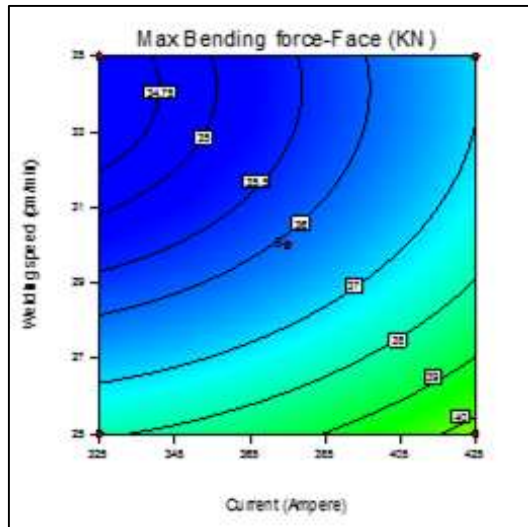**Figure 10: Predicted versus actual data**

Figure 11: 2D contour graph of maximum bending force as a function of welding speed and welding current
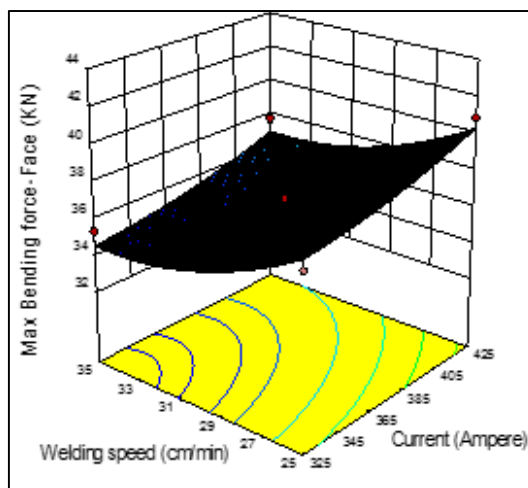

Figure 12: 3D surface plot of maximum bending force as a function of welding speed and welding current

Table 8: ANOVA for response surface quadratic model for hardness

Source	Sum of Squares	df	Mean Square	F Value	P-value Prob > F
Model	4274.59	4	1068.65	40.11	< 0.0001 significant
A-Current	751.19	1	751.19	28.20	0.0007
B-Welding speed	51.57	1	51.57	1.94	0.2016
AB	160.66	1	160.66	6.03	0.0396
A^2	208.53	1	208.53	7.83	0.0233
Residual	213.12	8	26.64		
Lack of Fit	150.61	4	37.65	2.41	0.2076 not significant
Pure Error	62.51	4	15.63		
Cor Total	4487.71	12			
Std. Dev.	5.16		R-Squared	0.9525	
Mean	181.05		Adj. R-Squared	0.9288	
C.V. %	2.85		Pred. R-Squared	0.8120	
PRESS	843.48		Adeq. Precision	19.155	

The final equation of harness terms of the actual factors is:

Hardness = +219.52183 - 0.29915 * Current + 6.45075 * Welding speed - 0.025350* Current * Welding speed +1.15702E-003 * Current^2 (3)

For checking statistically, the adequacy of the model, the normal probability plot (Figure 13) for the hardness data shows that the residuals generally fall on a straight line, revealing that the errors are normally distributed. In addition, from the residuals versus predicted responses plot (Figure 14) for the hardness results, it's noted that there are no clear patterns or uncommon structure, depicting that the models are accurate. Figure 15 manifests the predicted hardness versus the actual ones.

Figure 16 demonstrates the 2D contour plot of hardness in terms of welding current and travel speed. Referring to this figure, it can be noticed that the increment in current and travel speed individually causes a higher decrease in the hardness. The increase in the welding speed at lower current (325 Amp) resulted in more than (15 HV) decrease in hardness. Also, the increase in the current (425 Amp) at lower welding speed (25 cm/min) also resulted in a decrease in hardness. This means that both current and travel speed have a greater influence on the hardness individually and they proportionate inversely. Regarding the interaction of welding speed and current, this figure also shows that at (325 Amp and 25 cm/min), the combined influence of both factors gives a higher hardness (about 199 HV) than that caused by each one individually.

Figure 17 clarifies the 3D graph (surface plot) of hardness as a function of welding speed and current and confirms the observations mentioned in the 2D graph. One can observe that the increment of travel speed and current caused a decrease in the value of hardness at their higher level, whereas at their lower levels, they gave the highest value of hardness. This behavior is thought to be due to the thermal influence on the structure of the welded steel at both lower and higher levels. This agrees with ref. [2, 5, 6, 7, and 9].
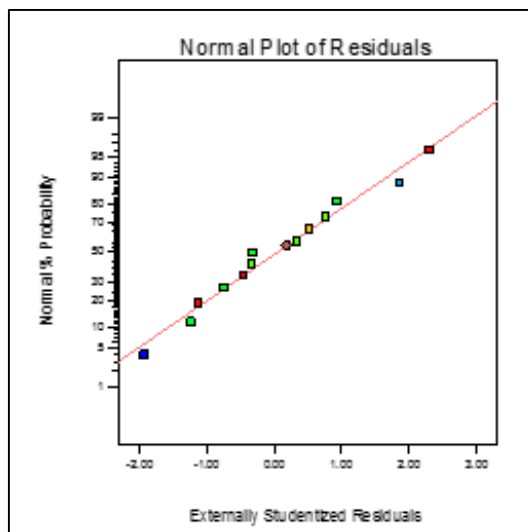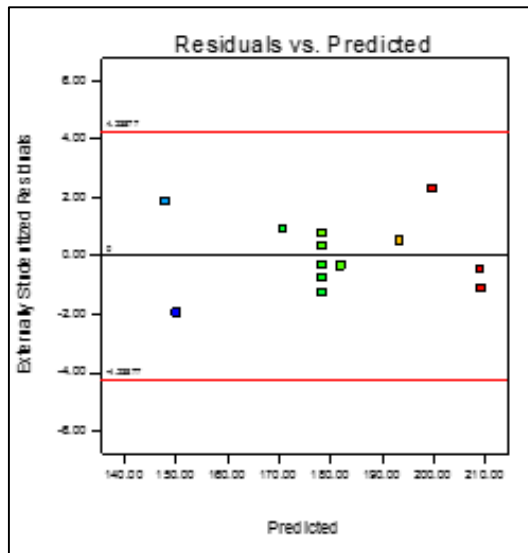

Figure 13: Normal distribution microhardness data
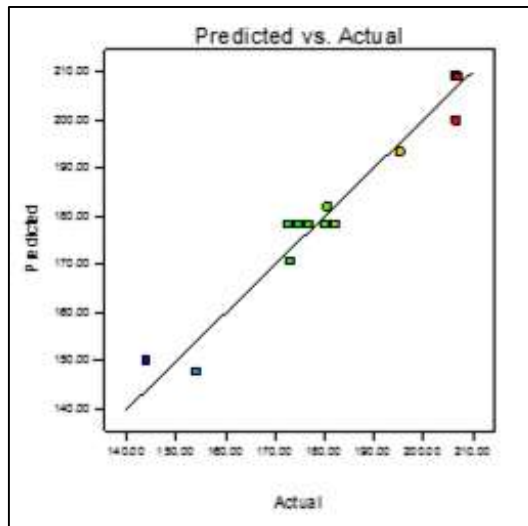
Figure 14: Residual versus predicted data

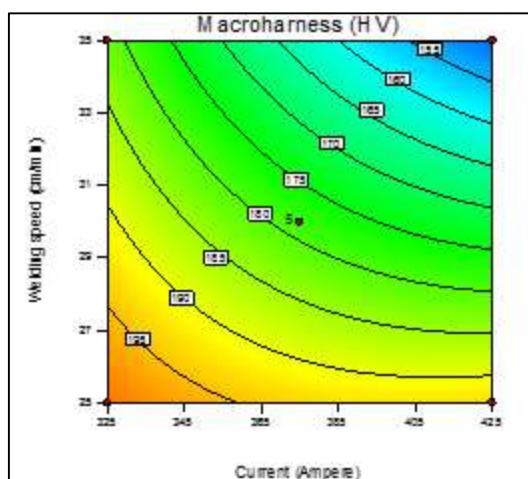**Figure 15: Predicted versus actual data**

Figure 16: 2D contour graph of hardness as a function of welding speed and welding current
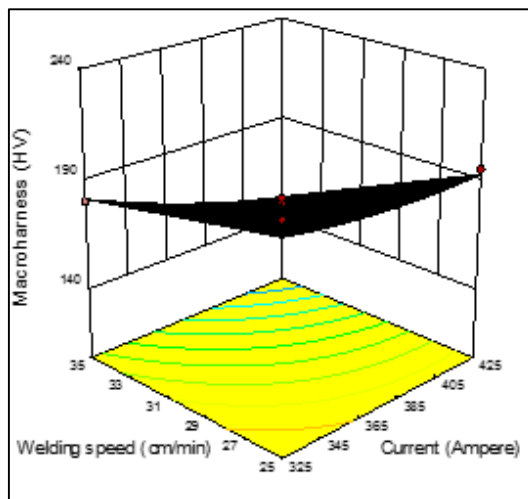
Figure 17: 3D surface plot of hardness as a function of welding speed and welding current

4. Optimization of Responses

Numerical optimization was employed by the DOE software using the results from Table 5 to obtain the optimum parameters combinations so as to achieve the desired needs, depending on the results from the predicted quadratic models for the mechanical properties as responses (yield stress, bending force and hardness) on terms of two input factors (current and travel speed).

The ultimate goal of such optimization was to find the maximum output (response) that at the same time satisfied all the changeable characteristics. Each variable constrains to optimize numerically the yield stress, bending force and hardness were used, and the input factors were selected for their used ranges, while the responses were selected to be the maximum for yield stress and bending force and minimum for hardness. Accordingly, one possible solution satisfied these constrains to find the desired values of the responses (474.447 MPa yield stress, 36.997 KN bending force and 150.065 HV hardness), as shown in Table 9 at the optimum values of welding current (425 Amp) and welding speed (35 cm/min).

5. Confirmation Tests at the Optimum Conditions

For checking the model's validity, confirmation tests were conducted at the optimum predicted results of the input factors determined in these models in order to measure the yield stress, bending force and hardness. The experimental measurements results are listed together with the predicted data in the table 10 for purpose of comparison. This table exhibits that the predicted and experimental results possess a good agreement according to the maximum error (1.05%, 1.92% and 4.25%) for yield stress, maximum bending force and hardness, respectively.

6. Joint Efficiency

The efficiency of the joint is a concept that exists in many (API) and (ASME) codes. It's a numerical value that is represented as a percentage, stated as the ratio of a welded, brazed or riveted joint strength to the base material strength. It's also a method for introducing the factors of safety in shells welding for the containment, and it can be written as following [13]:

$$Joint\ Efficiency\ E = \frac{Yield\ strength\ of\ weld}{Yield\ strength\ of\ base\ material} \qquad (4)$$

Depending on the yield strength values of the material before and after welding, the percentage of improvement in the joint efficiency was 24.5 %.

Table 9: The optimum values of input factors and responses

Welding current (Amp)	Welding speed (cm/min)	Yield stress (MPa)	Maximum bending force (KN)	Hardness (HV)
425	35	474.447	36.997	150.065

Table 10: Results of confirmation tests at the optimum conditions

Welding	Welding	Exp.	Pred.	Exp.	Pred.	Exp.	Pred.

current (Amp.)	speed (cm/min)	Yield Stress (MPa)	Yield Stress (MPa)	Maximum bending force (KN)	Maximum bending force (KN)	Hardness (HV)	Hardness (HV)
425	35	479.47	474.447	37.72	36.997	143.95	150.065
Error (%)		1.05		1.92		4.25	

4. Conclusions

1- Maximum yield stress occurred at higher level of welding speed and lower level of welding current.

2- The higher level of welding current and the lower level of welding speed gave the maximum value of bending force. However, the welding current was found not influential during welding over the used range of its levels.

3- The increase in both welding speed and current individually results in a higher decrease in the hardness, and both input factors proportionate inversely. Their combined effect at their lower levels gives the highest value of hardness.

References

[1] I. Gowrisankar, A. K. Bhaduri, V. Seetharaman, D. D. N. Verma, and D. R. G. Achar, "Effect of the number of passes on the structure and properties of submerged arc welds of AISI type 316L stainless steel," Weld. J., pp. 147–154, 1987.

[2] D. M. Viano, N. U. Ahmed, and G. O. Schumann, "Influence of heat input and travel speed on microstructure and mechanical properties of double tandem submerged arc high strength low alloy steel weldments," Sci. Technol. Weld. Join. Vol. 5, No. 1, pp. 26–34, 2000.

[3] A. M. Paniagua-Mercado, V. M. López-Hirata, and M. L. Saucedo Muñoz, "Influence of the chemical composition of flux on the microstructure and tensile properties of submerged-arc welds," J. Mater. Process. Technol., Vol. 169, No. 3, pp. 346–351, 2005.

[4] K. Prasad and D. K. Dwivedi, "Microstructure and tensile properties of submerged arc welded 1.25Cr-0.5Mo steel joints," Mater. Manuf. Process., vol. 23, no. 5, pp. 463–468, 2008.

[5] A. Harish, S. Kulwant, and S. Sanjay, "Cooling Rate Effect on Microhardness for SAW Welded Mild Steel Plate," Int. J. Theor. Appl. Res. Mech. Eng., vol. 2, No. 2, pp. 71–77, 2013.

[6] R. Kumar, H. K Arya, and S. RK, "Experimental determination of cooling rate and its effect on microhardness in submerged arc welding of mild steel plate (Grade c-25 as per IS 1570)," Mater. Sci. Eng., Vol. 03, No. 02, 2014.

[7] N. Singh, Karun, S. Kumar, and D. Singh, "Investigating the effect of saw parameters on hardness of weld metal," Int. J. Adv. Ind. Eng., Vol. 3, No. 2, pp. 68–74, 2015.

[8] S. A. Amin, S. H. Bakhy, and F. A. Abdullah, "Study the effect of welding parameters on the residual stresses induced by submerged arc welding process," Al-Nahrain J. Eng. Sci., Vol. 20, No. 4, pp. 945–951, 2017.

[9] S. H. Bakhy, S. A. Amin, and F. A. Abdullah, "Influence of SAW welding parameters on microhardness of steel A516-Gr60," Eng. Technol. J., Vol. 36, No. 10, pp. 1039–1047, 2018.

[10] ASME, ASME, BPVC, Sec. II: Materials, Part C: Specifications for welding rods, electrods and filler metals. The American Society of Mechanical Engineers, 2015.

[11] ASME, ASME, BPVC, Sec.II: Materials, Part A: ferrous material specifications (SA-451 to End). The American Society of Mechanical Engineers, 2015.